NONOSCILLATORY ADVECTION SCHEMES

Piotr K. Smolarkiewicz
National Center for Atmospheric Research[1]
Boulder, Colorado 80307 USA

Summary: This paper discusses selected topics in the area of nonoscillatory advection schemes. These include stability properties of sign-preserving schemes, design and degrees of freedom of flux-corrected-transport (FCT) monotonicity-preserving schemes, and implementation of the nonoscillatory advection schemes as interpolation operators in semi-Lagrangian approximations for atmospheric fluids.

1. INTRODUCTION

One complaint against traditional numerical methods for advection transport is that they usually lead to negative values in the positive-definite scalar fields (e.g., water substance, chemical tracers) or, in more general terms, to spurious numerical over- and undershots in regions of steep gradients in these variables. Such numerical noise, which may be acceptable where advection is the only concern, may lead to large errors in nonlinear interactions between the two advected scalars (e.g., where small negative value multiplies large positive value — as may happen, for instance, in chemical reactions or phase-change processes). Traditional techniques that are free of these problems are only first-order-accurate and exhibit a tendency to overly diffuse numerical solutions. In the last two decades, advanced finite-difference methods for solving the transport problem have been designed that are essentially free of the spurious oscillations characteristic of higher-order methods yet do not suffer from the excessive implicit diffusion characteristic of low-order methods (see Sweby, 1984; Zalesak, 1987; Smolarkiewicz and Grabowski, 1990, for reviews and discussions). Although these essentially nonlinear algorithms are far more complex than the traditional linear schemes, they offer strong (linear and nonlinear) stability, maintain steep gradients of the transported fields, and preserve the monotonicity and/or sign of the advected variable. These properties make them potentially attractive tools for applications which combine transport with processes responsible for coupling the advected variables.

[1] The National Center for Atmospheric Research is sponsored by the National Science Foundation

The majority of existing nonoscillatory methods [also referred to as monotonicity or shape preserving, shock capturing, total variation diminishing (TVD), or briefly, monotone schemes[1]] were designed keeping in mind the applications to shock-forming flows. Such applications demand from numerical methods certain specific properties that are not necessarily essential in typical atmospheric problems. In atmospheric applications, methods suppressing spurious oscillations are usually considered in the context of advection transport equations; and their most advertised properties are sign-preservation and the overall smooth appearance of the solutions. In applications addressing shock-forming flows, nonoscillatory techniques are usually discussed in the context of the conservation laws of compressible gas dynamics, and the focus of interest is on the convergence of numerical approximations to the unique, physically relevant solution (cf. Harten et al., 1976; Merriam, 1989). Although the theory of TVD methods for scalar conservation laws has been considerably advanced during the last decade, so far it has had a limited impact upon the development of numerical methods in the area of meteorology. One reason for this is that systems of equations modeling natural atmospheric phenomena appear far more complex than idealized conservation laws that are of concern in the area of theoretical, numerical analysis. Complexity of atmospheric equations associated with multidimensionality, earth rotation, sphericity, orography, phase-change processes, radiation, chemical reactions, and other natural effects makes stability, second-order accuracy, generality, and computational efficiency the primary concerns of atmospheric models.

Keeping in mind the practical needs of meteorology, we shall address in this paper selected nonoscillatory methods for advection transport equations that have proven useful in a variety of complex atmospheric applications. The intention of this lecture is to expose those underlying concepts common to many nonoscillatory methods that are universally applicable to arbitrary atmospheric flows.[2] Further in this paper, we shall take the freedom of recognizing sign-preserving algorithms as a class of

[1] This nomenclature, popular in applications, is somewhat misleading as it mixes terms that in the mathematical literature may have different precise meanings (e.g., monotone and monotonicity preserving schemes; see Harten, 1983).

[2] Although there is a wide availability of nonoscillatory techniques suitable for constant-coefficient advection in one spatial dimension, there are few techniques adequate for general flows.

nonoscillatory methods[3] as they are particularly important for atmospheric applications and employ certain general concepts inherent in advanced nonlinear techniques. In order to emphasize that there is more to nonoscillatory advection schemes than just sign-preservation and smooth appearance of approximate solutions, we shall discuss in the following section the stability properties of nonoscillatory schemes. Section 3 deals in some detail with the principles and degrees of freedom of monotonicity-preserving flux-corrected-transport (FCT) methods (the original TVD schemes) whose derivatives are becoming increasingly more popular in meteorological modeling. Section 4 addresses a particular class of applications, where simple, one-dimensional monotone transport algorithms suitable for integrating a constant-coefficient advection equation play the role of interpolation operators in semi-Lagrangian approximations for an arbitrary atmospheric-fluid system.

2. COMPUTATIONAL STABILITY OF NONOSCILLATORY ADVECTION SCHEMES

The basic equation to be solved is the continuity equation describing the transport of a nondiffusive scalar quantity in M-dimensional space,

$$\frac{\partial \psi}{\partial t} + \sum_{I=1}^{M} \frac{\partial}{\partial x^I}(\psi u^I) = 0, \tag{1}$$

where $\psi \equiv \psi(t, x^1, .., x^M)$ is the nondiffusive scalar quantity; $u^I \equiv u^I(t, x^1, .., x^M)$ is the I^{th} velocity component, $I = 1, ..., M$; and $t, \mathbf{x} \equiv (x^1, ..., x^M)$ are the time- and space-independent variables. In order to compress the notation in the following numerical equations, we choose traditional n and $\mathbf{i}$ indices to denote, respectively, the temporal and spatial position on a uniform computational grid $(t^n, \mathbf{x_i}) = (n\Delta t, i_1 \Delta X^1, .., i_M \Delta X^M)$; and adopt $\mathbf{e}_I$ for the unity vector in the I direction [i.e., $\mathbf{e}_I = (0, .., 1, .., 0)$ with 1 appearing at the I position]. A conservative advection algorithm for integration of (1) may then be compactly written as:

$$\psi_{\mathbf{i}}^{n+1} = \psi_{\mathbf{i}}^{n} - \sum_{I=1}^{M} \left(F^I_{\mathbf{i}+1/2\mathbf{e}_I} - F^I_{\mathbf{i}-1/2\mathbf{e}_I} \right), \tag{2}$$

[3] In general, the sign-preserving schemes are subject to spurious over- and undershooting; however, they are usually nonoscillatory near "zeros" of the transported variable.

where $F^I_{\mathbf{i}+1/2\mathbf{e}_I}\Delta X^I$ is an approximation to the I component of the integrated advective flux, evaluated at $\mathbf{i}+\frac{1}{2}\mathbf{e}_I$ position on the grid based on the information provided in a local neighborhood of the $\mathbf{i}+\frac{1}{2}\mathbf{e}_I$ grid point. Since in (2) the time level of the fluxes may be taken at any position, this equation represents the general form of an arbitrary finite-difference flux-form scheme. For the sake of illustration, the fluxes from selected, elementary, one-dimensional advection schemes are explicitly written as follows:

$$F_{i+1/2} = [\alpha^n_{i+1/2}]^+\psi^n_i + [\alpha^n_{i+1/2}]^-\psi^n_{i+1} \ , \tag{3a}$$

$$F_{i+1/2} = \frac{1}{2}\alpha^n_{i+1/2}(\psi^n_{i+1}+\psi^n_i) - \frac{1}{2}(\alpha^n_{i+1/2})^2(\psi^n_{i+1}-\psi^n_i) \ , \tag{3b}$$

$$F_{i+1/2} = \frac{1}{2}\alpha^{n+1/2}_{i+1/2}(\psi^{n+1/2}_{i+1}+\psi^{n+1/2}_i) \ , \tag{3c}$$

where $\alpha \equiv \frac{u\Delta t}{\Delta X}$ is a local Courant number, defined on a staggered grid, and $[\ ]^+$, $[\ ]^-$ denote the nonnegative- and nonpositive-part operators, respectively. Equations (3a-c) provide fluxes from, correspondingly, the first-order-accurate donor-cell (alias upwind, upstream) scheme, the second-order-accurate (for uniform flow) Lax-Wendroff scheme,[4] and the second-order-accurate, centered-in-time-and-space (leap-frog) scheme. A simple, compact form of the advective fluxes in (3a-c) is typical of elementary advection schemes. The nonoscillatory methods yield complex fluxes that often require several equations for their explicit representation. An example of such a method will be discussed in the next section, while further in this section we shall investigate the stability properties common to many nonoscillatory methods regardless of their explicit formulation.

In order to assess the computational stability of nonoscillatory schemes, consider first a *constant-sign* field $\psi(t,\mathbf{x})$ in (1) and an arbitrary, sign-preserving advection algorithm in (2). For simplicity, assume that both analytic and numerical fluxes vanish at the boundaries of a computational domain. Then, the conservation form of (2) implies

$$\underset{n}{\forall} \ \sum_{\mathbf{i}} \psi^n_{\mathbf{i}} = \sum_{\mathbf{i}} \psi^0_{\mathbf{i}} \ . \tag{4}$$

[4] See the accompanying paper in this volume for a detailed discussion of this scheme as well as its extensions and derivatives.

Since the scheme preserves the sign of the transported quantity by assumption, (4) is equivalent to

$$\underset{n}{\forall} \quad \sum_i |\psi_i^n| = \sum_i |\psi_i^0| \,. \tag{5}$$

Recalling that $\sum |\ | \geq (\sum(\ )^2)^{\frac{1}{2}}$, (5) implies that

$$\underset{n}{\forall} \quad \sum_i (\psi_i^n)^2 \leq \Big(\sum_i |\psi_i^0|\Big)^2 \equiv \mathcal{B} \,. \tag{6}$$

In other words, total "energy" ("entropy") of the sign-preserving solution is uniformly bounded in time, which is to say that the sign-preserving solution is computationally stable. Since for a sufficiently small time step advection schemes can be designed which are sign-preserving for arbitrary flows (e.g., Smolarkiewicz, 1984; Smolarkiewicz and Clark, 1986), the inequality in (6) is a statement of both linear and nonlinear stability for such schemes.

The simplicity of the result in (6) is a direct consequence of the assumption that ψ is of a constant sign. For variable-sign fields, a similar result may be obtained by noting that every ψ may be uniquely decomposed into the nonpositive and nonnegative part, $\psi = [\psi]^+ + [\psi]^-$. Since the two parts have disjoined supports, they are independent of each other, and they both satisfy (1). Applying a sign-preserving advection scheme to both parts ensures uniform boundedness of both $[\psi]^+$ and $[\psi]^-$, and consequently of their sum. Such arguments can be further elaborated (over a single time step) for the transport equation with forcings and/or sources leading to the conclusion that *sign-preserving advection schemes*[5] *offer the means of controlling nonlinear stability in numerical models.* This result is rarely appreciated in the meteorological literature, where sign- and/or shape-preserving schemes are usually considered in the context of their elementary (defining) properties, and where Arakawa-type schemes (Arakawa, 1966) are thought to be the obvious choice insofar as the nonlinearly stable, finite-difference advection transport algorithms are concerned.

[5] This also concerns monotonicity-preserving schemes, as every monotonicity-preserving scheme is also sign-preserving (the opposite is not true).

3. GENERAL FCT PROCEDURE

Among a variety of existing *monotonicity-preserving* methods, the FCT schemes originated by Boris and Book (1973), and later generalized to fully multidimensional algorithms by Zalesak (1979), become perhaps the only modern nonlinear approach that has been adopted on a permanent basis in several atmospheric and oceanic research models. It is important to realize that FCT is a general concept that allows several degrees of freedom and may lead to many different schemes. A number of known nonoscillatory techniques may be viewed as either a particular realization of the FCT approach or as implementing certain conceptual elements of FCT in their design (see Sweby, 1984, and Zalesak, 1987, for discussions). The basic idea of the FCT approach is simple: The generic reason for the appearance of the oscillations in the numerically generated higher-order-accurate solutions to (1) is that the magnitude of certain fluxes is overestimated with respect to their analytic value. In contrast, the magnitude of the fluxes given by the first-order-accurate schemes is underestimated, which results in monotone but heavily damped solutions (Zalesak, 1979). The FCT procedure overcomes the problem of false oscillations by imposing appropriate limits on the transport fluxes from the higher-order-accurate algorithms. In order to expose the degrees of freedom and the assumptions invoked, we discuss below the essential aspects of the general FCT scheme.

Consider an arbitrary, higher-order-accurate advection algorithm for the integration of (1):

$$\psi_{\mathrm{i}}^{n+1} = \psi_{\mathrm{i}}^{n} - \sum_{I=1}^{M} \left(FH^{I}_{\mathrm{i}+1/2\mathbf{e}_I} - FH^{I}_{\mathrm{i}-1/2\mathbf{e}_I} \right) . \tag{7}$$

The high-order FH-flux may be arbitrarily cast into the sum of the flux from a certain low-order nonoscillatory scheme and the residual, i.e.,

$$FH^{I}_{\mathrm{i}+1/2\mathbf{e}_I} \equiv FL^{I}_{\mathrm{i}+1/2\mathbf{e}_I} + A^{I}_{\mathrm{i}+1/2\mathbf{e}_I} , \tag{8}$$

where (8) defines the residual A-flux, which has a sense of correcting *at least* the first-order truncation error terms in the transport fluxes of the low-order scheme, i.e.,

$$A^{I}_{\mathrm{i}+1/2\mathbf{e}_I} \sim \Delta t \cdot \mathcal{O}(\Delta X, \Delta t) + HOT , \tag{9}$$

where *HOT* has the usual meaning of "higher order terms". Because of this compensation of the leading truncation-error term in a low-order scheme, the A-flux is traditionally referred to as the "antidiffusive" flux. Using (8) in (7) results in

$$\psi_{\mathbf{i}}^{n+1} = \Psi_{\mathbf{i}}^{n+1} - \sum_{I=1}^{M} \left(A^I_{\mathbf{i}+1/2\mathbf{e}_I} - A^I_{\mathbf{i}-1/2\mathbf{e}_I} \right) , \tag{10}$$

where "Ψ" denotes the solution given by the low-order scheme, which by assumption satisfies

$$\psi_{\mathbf{i}}^{MAX} \geq \Psi_{\mathbf{i}}^{n+1} \geq \psi_{\mathbf{i}}^{MIN} , \tag{11}$$

where $\psi_{\mathbf{i}}^{MAX}$ and $\psi_{\mathbf{i}}^{MIN}$ are yet unspecified maximal and minimal values of the scalar within the $\mathbf{i}^{th}$ grid box that achieve the monotonicity of the scheme. Their explicit form will be discussed later in this section. Inasmuch as $\Psi_{\mathbf{i}}^{n+1}$ preserves the monotone character of the transported field [by means of (11)], the eventual oscillatory behavior in $\psi_{\mathbf{i}}^{n+1}$ comes from overestimating the magnitude of certain A-fluxes in (10). Thus, to ensure ripple-free solutions it is sufficient to appropriately limit A-fluxes such that

$$\tilde{A}^I_{\mathbf{i}+1/2\mathbf{e}_I} = C^I_{\mathbf{i}+1/2\mathbf{e}_I} \cdot A^I_{\mathbf{i}+1/2\mathbf{e}_I} , \tag{12}$$

where C-coefficients, that in general are functions of the low- and high-order solutions on the grid, are determined from the set of constraints

$$0 \leq C^I_{\mathbf{i}+1/2\mathbf{e}_I} \leq 1 \tag{13}$$

and

$$\psi_{\mathbf{i}}^{MAX} \geq \tilde{\psi}_{\mathbf{i}}^{n+1} = \Psi_{\mathbf{i}}^{n+1} - \sum_{I=1}^{M} \left(\tilde{A}^I_{\mathbf{i}+1/2\mathbf{e}_I} - \tilde{A}^I_{\mathbf{i}-1/2\mathbf{e}_I} \right) \geq \psi_{\mathbf{i}}^{MIN}. \tag{14}$$

When $C^I_{\mathbf{i}+1/2\mathbf{e}_I}$ is equal to zero or unity[6] the resulting transport flux in (14) becomes $FL^I_{\mathbf{i}+1/2\mathbf{e}_I}$ or $FH^I_{\mathbf{i}+1/2\mathbf{e}_I}$, respectively. The assumed convergence of the low-order schemes involved in (8) together with (9), (12), and (13) ensure the convergence of the $\tilde{\psi}$-solutions in (14) as $\Delta X, \Delta t \longrightarrow 0$.

The constraints in (13) and (14) allow one to derive formally (see Smolarkiewicz and Grabowski, 1990, for the step-by-step solution of the constraining inequalities)

[6] In some nonoscillatory schemes, a more generous upper limit is considered (Sweby, 1984).

the explicit form of the C-coefficients and, consequently, the explicit form of the limited antidiffusive fluxes in (12). The derivation provides maximized $\tilde{A}$-fluxes in (12) satisfying constraints (13) and (14):

$$\tilde{A}^I_{\mathbf{i}+1/2\mathbf{e}_I} = min\left(1, \beta^{\downarrow}_{\mathbf{i}}, \beta^{\uparrow}_{\mathbf{i}+\mathbf{e}_I}\right)\left[A^I_{\mathbf{i}+1/2\mathbf{e}_I}\right]^+ + min\left(1, \beta^{\uparrow}_{\mathbf{i}}, \beta^{\downarrow}_{\mathbf{i}+\mathbf{e}_I}\right)\left[A^I_{\mathbf{i}+1/2\mathbf{e}_I}\right]^- , \quad (15)$$

where

$$\beta^{\uparrow}_{\mathbf{i}} \equiv \frac{\psi^{MAX}_{\mathbf{i}} - \Psi^{n+1}_{\mathbf{i}}}{A^{IN}_{\mathbf{i}} + \varepsilon} \; ; \quad \beta^{\downarrow}_{\mathbf{i}} \equiv \frac{\Psi^{n+1}_{\mathbf{i}} - \psi^{MIN}_{\mathbf{i}}}{A^{OUT}_{\mathbf{i}} + \varepsilon} , \quad (16a, b)$$

and $A^{IN}_{\mathbf{i}}$, $A^{OUT}_{\mathbf{i}}$ are the absolute values of the total incoming and outgoing A-fluxes from the $\mathbf{i}^{th}$ grid box, $A^{IN}_{\mathbf{i}} \equiv \sum_{I=1}^{M}\left([A^I_{\mathbf{i}-1/2\mathbf{e}_I}]^+ - [A^I_{\mathbf{i}+1/2\mathbf{e}_I}]^-\right)$ and $A^{OUT}_{\mathbf{i}} \equiv \sum_{I=1}^{M}\left([A^I_{\mathbf{i}+1/2\mathbf{e}_I}]^+ - [A^I_{\mathbf{i}-1/2\mathbf{e}_I}]^-\right)$, respectively. ε is a small value, e.g., $\sim 10^{-15}$, which has been introduced herein to allow for efficient coding of β-ratios when $A^{IN}_{\mathbf{i}}$ or $A^{OUT}_{\mathbf{i}}$ vanish. The equations (14), (15), (8), and (16a, b) constitute a general, arbitrary dimensional form of the FCT algorithm discussed by Zalesak (1979) (his formulas 14, 14′ are not required to preserve monotonicity and, in my experience, may cause certain pathological behaviors of the FCT schemes). The arbitrary dimensionality of this procedure contrasts with the alternate-direction approach utilized by most other monotone schemes.

In order to determine $\beta^{\uparrow}_{\mathbf{i}}$ and $\beta^{\downarrow}_{\mathbf{i}}$ uniquely, one must specify the limiter $\psi^{MAX}_{\mathbf{i}}$, $\psi^{MIN}_{\mathbf{i}}$ in (16a, b). The simple, standard limiter (Zalesak, 1979) is

$$\psi^{MAX}_{\mathbf{i}} = \max_I\left(\psi^n_{\mathbf{i}-\mathbf{e}_I}, \psi^n_{\mathbf{i}}, \psi^n_{\mathbf{i}+\mathbf{e}_I}, \Psi^{n+1}_{\mathbf{i}-\mathbf{e}_I}, \Psi^{n+1}_{\mathbf{i}}, \Psi^{n+1}_{\mathbf{i}-\mathbf{e}_I}\right) \quad (17a)$$

$$\psi^{MIN}_{\mathbf{i}} = \min_I\left(\psi^n_{\mathbf{i}-\mathbf{e}_I}, \psi^n_{\mathbf{i}}, \psi^n_{\mathbf{i}+\mathbf{e}_I}, \Psi^{n+1}_{\mathbf{i}-\mathbf{e}_I}, \Psi^{n+1}_{\mathbf{i}}, \Psi^{n+1}_{\mathbf{i}-\mathbf{e}_I}\right). \quad (17b)$$

The low-order, nonoscillatory Ψ-solutions appearing in (17a, b) constitute the original limiter of Boris and Book (1973). This limiter effectively prevents development of spurious oscillations in an arbitrary flow field. Zalesak (1979) extended the original limiter onto the local extrema of the solution at the previous time step. The goal of this extension is to improve the predictions in incompressible flows where the only extrema allowed in an arbitrary grid point are those that were present in its immediate environment (determined by the CFL stability criteria) at the previous time step; in principle, i.e., with accuracy to round-off errors, the original Boris and Book

limiter is redundant in incompressible flows (which is a common case in meteorological applications). Note that the limiters in (17) ensure uniform boundedness of the solution, providing uniformly bounded Ψ. Since uniform boundedness of the low-order solutions is easily achievable, a nonlinear stability of the FCT approximations is assured essentially by design. Note also that the FCT limiters in (17) impose tighter bounds on the finite difference solutions than the "energy" ("entropy") constraint (6) of sign-preserving schemes considered in the preceding section.

There are several degrees of freedom in the approach outlined. First, the constraints (13) and (14) can be supplemented with some additional conditions which may need to be satisfied by a final approximation. This degree of freedom has been exploited in Grabowski and Smolarkiewicz (1990), where constraints (13) and (14) for the temperature and water substance fields advected in a cloud model were supplemented with a requirement that the diagnosed field of relative humidity and, therefore, a solution to a complete advection-condensation cycle also remain nonoscillatory. Second, so long as (11) holds, the limiters themselves may be, in principle, arbitrary.[7] This degree of freedom is particularly useful where synchronized limiting of a system of equations is concerned (see for example Grabowski and Smolarkiewicz, 1990). Finally, the third degree of freedom is in the choice of the high- and low-order schemes mixed by the FCT procedure. As there are no essential restrictions imposed on the mixed schemes, a variety of FCT algorithms may be designed.[8]

Insofar as the atmospheric applications are concerned, Ψ evaluated with the first-order-accurate upwind scheme is usually considered as a low-order solution,[9] whereas the leap-frog advection schemes are usually selected (following Zalesak, 1979) for the high-

[7] This emphasizes that a nonoscillatory character of the solutions is understood in a relative sense with respect to Ψ and the limiters, and that the limiters essentially define "monotonicity" of the resulting FCT scheme (for instance, selecting weaker limiters $\psi_i^{MAX} = \infty$ and $\psi_i^{MIN} = 0$ leads to positive-definite, but apparently oscillatory, advection schemes).

[8] The formalism outlined does not necessarily require mixing of low- and high-order schemes but provides a general framework for mixing any two algorithms attractive for a particular problem at hand.

[9] In applications addressing shock-forming flows, implicit diffusivity of the upwind scheme may be insufficient to ensure smooth solutions, and more diffusive low-order schemes may need to be considered (cf. Zalesak, 1979).

order-accurate algorithms.[10] However, as the resulting FCT algorithm mixes the two schemes of different distributions of the truncation errors, it is not necessarily optimal in terms of overall accuracy. The leap-frog schemes yield excellent amplitude behavior but large phase errors, whereas the upwind scheme suffers from large amplitude errors but relatively small phase errors. Because the low- and high-order solutions are shifted in phase, the FCT mixing of the two solutions (which should eliminate dispersive ripples essentially without degrading the accuracy of the high-order solutions) is inefficient.

The latter point is illustrated in Fig. 1a, which shows the results of one-dimensional uniform advection of the irregular signal (heavy solid line; see Smolarkiewicz and Grabowski, 1990, for details). The dashed line corresponds to the leap-frog solution, whereas the thin solid line displays the solution obtained with the upwind/leap-frog FCT scheme. Although the FCT procedure efficiently removes the dispersive ripples, the amplitudes of the initial perturbations are severely damped at the cost of improving the phase error. The overall accuracy of the FCT solutions may be improved by employing for the high-order scheme an algorithm of phase-error characteristics similar to those of the low-order scheme. The nonlinear MPDATA methods (already outlined in section 3 of the accompanying paper in this volume) are an excellent choice for this purpose as they yield phase-errors similar to those in the upwind scheme (Smolarkiewicz and Clark, 1986). The MPDATA schemes, whose design is conceptually unrelated to the FCT approach, are at least second-order-accurate for arbitrary flows and already preserve the sign of the transported field (therefore, for many practical applications they do not require additional FCT enhancement). Figure 1b shows the MPDATA solution (dashed line) and the fully nonoscillatory solution obtained with the FCT version of this scheme (thin solid line), as well as the analytic solution (heavy solid line). Comparison of the three curves shows that the primary effect of the FCT modification is to remove the overshoot and the undershoot present in the original MPDATA solution. Neither of the solutions in Figs. 1a and 1b is capable of capturing the fine details of the initial condition. This aspect of the solutions may be improved (Fig. 1c) by exploiting the fourth-order-accurate dissipative scheme of Tremback et al. (1987) as the high-order

[10] Such a choice appears natural in the context of multidimensional procedure, as leap-frog schemes are both simple and second-order-accurate in arbitrary flows.

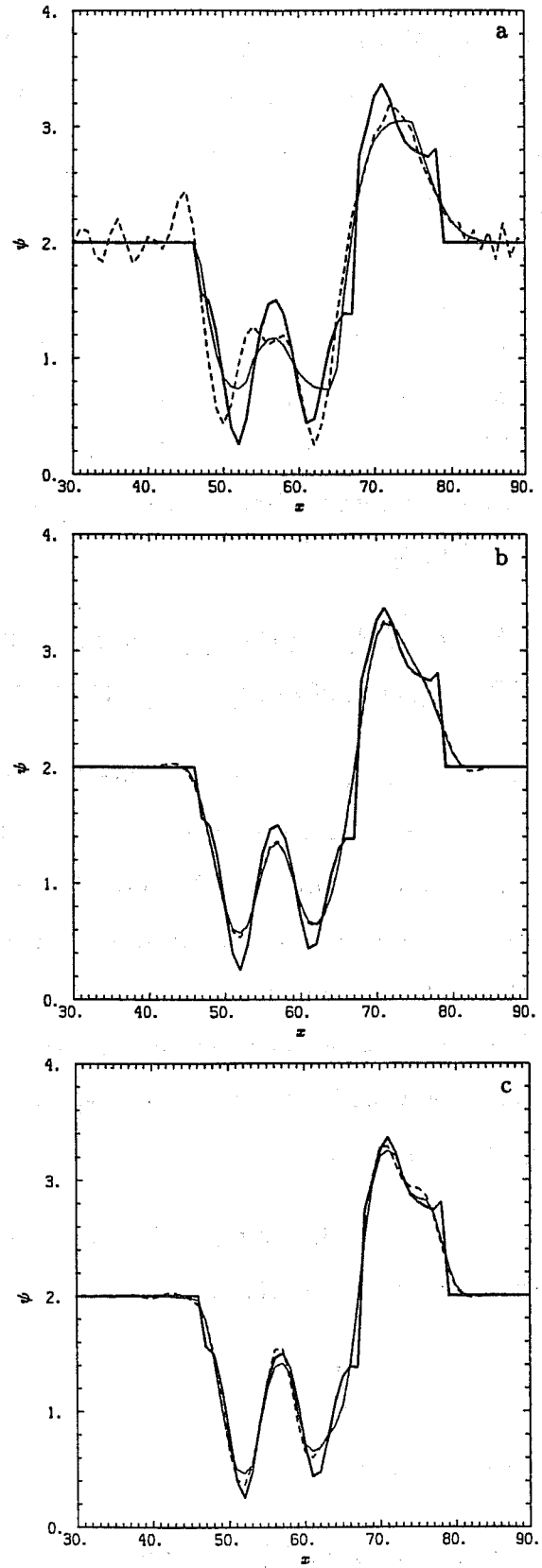

Figure 1. Uniform advection of the irregular signal (heavy solid lines) with oscillatory schemes (dashed lines) and their nonoscillatory, FCT versions (thin solid lines): a) the second-order-accurate leap-frog scheme, b) the second-order-accurate MPDATA, and c) the fourth-order-accurate dissipative scheme of Tremback et al. (1987).

scheme in the FCT procedure. However, this result is somewhat deceiving as the employed algorithm achieves its formal accuracy only for one-dimensional, constant-coefficient advection equations (for discussion, see the accompanying paper in this volume) and therefore is not universally attractive for applications with complex natural flows.

The simple example discussed has illustrated only the most elementary aspects of the FCT approach. The reader interested in a more elaborate discussion of accuracy and efficiency of FCT schemes, as well as in applications representative of natural atmospheric problems, is referred to Smolarkiewicz and Grabowski (1990), and Grabowski and Smolarkiewicz (1990).

4. SEMI-LAGRANGIAN APPROXIMATIONS TO ATMOSPHERIC FLUIDS USING NONOSCILLATORY ADVECTION SCHEMES

Having established general FCT procedure and its degrees of freedom, we shall narrow the discussion herein to a special class of applications which emphasizes the utility and importance of all those one-dimensional nonoscillatory schemes which are suitable for integrating merely a constant-coefficient advection equation. Although such schemes are not particularly competitive in applications addressing complex natural problems in Eulerian formulation, they become accurate and powerful tools as nonoscillatory interpolation operators inherent in semi-Lagrangian representation of equations governing atmospheric phenomena.

The notion of a semi-Lagrangian approach is simple. It originates with a Lagrangian form of the evolution equation for a fluid variable ψ

$$\frac{d\psi}{dt} = R \tag{18}$$

and the particular interpretation of its integral

$$\psi(\mathbf{x}_i, t) = \psi(\mathbf{x}_o, t_o) + \int_T \mathcal{R} dt \ , \tag{19}$$

where $(\mathbf{x}_i, t)$ and $(\mathbf{x}_o, t_o)$ are the two points connected by a parcel's trajectory T, and R combines all sources and forces. Assuming that $(\mathbf{x}_i, t)$ represents points of a

regular mesh, one computes backward-in-time the trajectories arriving at $(\mathbf{x}_i, t)$ and finds their departure points $(\mathbf{x}_o, t_o)$. Since the departure points do not necessarily coincide with the points of the mesh, information therein is not immediately available, and one has to invoke an interpolation procedure to determine $\psi(\mathbf{x}_o, t_o)$. In essence, similar action must be taken with respect to the source term, with details depending upon a selected method of the integral's approximation and the particular problem at hand. The backward-in-time integration of the trajectories and the nonconservative form of the governing equations make the approach distinct from a class of mixed arbitrary-Lagrangian-Eulerian (ALE) methods (Hirt et al., 1974) popular in the area of computational fluid dynamics. The advertised advantages of semi-Lagrangian techniques are a circumvention of the CFL stability condition (typical of Eulerian methods) and the convenience of a regular-mesh discretization (contrasting with purely Lagrangian techniques). A variety of semi-Lagrangian methods has been designed exploiting different interpolation techniques and different temporal discretizations (see Staniforth and Côté, 1991, for a review).

The recent work of Smolarkiewicz and Rasch (1990) suggests that semi-Lagrangian methods represent a special case of a more general approach. Referring to elementary properties of differential forms and viewing a ψ variable as a 0-form on the time-space continuum, one can relate two values of the variable at any two points of the continuum through the Stokes' theorem, gaining thereby a large degree of freedom associated with the selection of points and connecting contours. Selecting contours whose elements coincide with parcels' trajectories leads to a variety of semi-Lagrangian formulations. Moreover, this approach documents that interpolation procedures — inherent to semi-Lagrangian approximations — may be replaced with Eulerian algorithms suitable for integrating constant-coefficient advection equations while retaining their formal accuracy and such attractive properties as monotonicity and/or sign preservation. In order to show this latter point (which is of particular interest to applications), consider the following interpolation problem: Let us assume that at an arbitrary instance t_o (for conciseness, the dependence of ψ on t_o will be dropped in the following discussion) a sufficiently continuous field $\psi : \mathbf{R}^M \longrightarrow \mathbf{R}^1$ is known *a priori* in $\mathbf{x}_i$ points of a uniform mesh in $\mathbf{R}^M$. For the sake of clarity, we restrict ourselves to regular meshes with a

constant grid interval $\Delta\mathbf{X} \equiv (\Delta X^1, ..., \Delta X^M)$ such that $\mathbf{x_i} = \mathbf{i} \circ \Delta\mathbf{X}$. The problem addressed is to provide an estimate of ψ, with certain desired accuracy, in a point of interest $\mathbf{x}_o$ noncoincident, in general, with any of $\mathbf{x_i}$'s. The traditional approach is to expand ψ in, say, the p-th order Taylor sum about some $\mathbf{x_i}$ from a local neighborhood of $\mathbf{x}_o$ and provide adequate estimates of the derivatives using information available on the grid, or, equivalently, to evaluate ψ at $\mathbf{x}_o$ based on the assumption that ψ fits a p-th order Lagrangian polynomial in between the grid points (cf. Tremback et al., 1987). Consider, however, an alternate approach.

As a consequence of the Stokes' theorem,

$$\psi(\mathbf{x}_o) - \psi(\mathbf{x_i}) = \int_C d\mathbf{x} \circ \nabla\psi(\mathbf{x}) \ , \tag{20}$$

where C denotes an arbitrary contour connecting the point of interest $\mathbf{x}_o$ with an arbitrary $\mathbf{x_i}$ of the computational grid. Exploiting the arbitrariness of the contour selection in (20), we choose for C a line segment of the parametric equation

$$\mathbf{x}(\mathbf{x_i}, \tau) = -(\mathbf{x_i} - \mathbf{x}_o)\tau + \mathbf{x_i} \ , \tag{21}$$

where the parameter $\tau \in [0, 1]$. Implementing (21) in (20) gives

$$\phi(\mathbf{x_i}, 1) = \phi(\mathbf{x_i}, 0) - \int_0^1 (\mathbf{x_i} - \mathbf{x}_o) \circ \nabla\phi(\mathbf{x_i}, \tau) d\tau \ , \tag{22}$$

where

$$\phi(\mathbf{x_i}, \tau) \equiv \psi\big(\mathbf{x}(\mathbf{x_i}, \tau)\big) \ . \tag{23}$$

Since for fixed $\mathbf{x}_o$ and $\mathbf{x_i}$, the first element of the scalar product appearing under the integral in (22) is constant, (22) may be rewritten as

$$\phi(\mathbf{x_i}, 1) = \phi(\mathbf{x_i}, 0) - \int_0^1 \nabla \circ \big(\mathbf{U}\phi\big)(\mathbf{x_i}, \tau) d\tau \ , \tag{24}$$

where

$$\mathbf{U} \equiv \mathbf{x_i} - \mathbf{x}_o \ . \tag{25}$$

Although (24) can be obtained alternatively from the *untruncated* Taylor formula (Smolarkiewicz and Grell, 1991), the current derivation is more general as it exposes

the degree of freedom associated with a contour selection in (21); in particular, selecting the contour consisting of a sequence of the line segments parallel to spatial coordinates leads to the alternate-direction (time-split) representation of (24).

Equation (24) represents the integral of the equation

$$\frac{\partial \phi}{\partial \tau} + \nabla \circ (\mathbf{U}\phi) = 0 \tag{26}$$

over the τ interval $[0,1]$ at $\mathbf{x_i}$ grid-point. In other words, (24) is a formal solution to the advection equation (26) in which the free parameter τ plays the role of a time independent variable, and the vector $\mathbf{U}$ defined in (25) plays the role of the velocity field. Therefore, the interpolation problem has been expressed as the equivalent advection problem, and (24) may be approximated using, in principle, any known advection algorithm. Among the variety of available advection algorithms, the forward-in-time schemes are the most attractive for applications, as they require information only from $\mathbf{x}(\mathbf{x_i}, \tau = 0)$ points in (21), where $\phi(\mathbf{x_i}, 0) = \psi(\mathbf{x_i})$ are known by assumption. Such an approximation may be compactly written as

$$\phi_{\mathbf{i}}^1 = \phi_{\mathbf{i}}^0 - \mathcal{AS}_{\mathbf{i}}(\phi^0, \boldsymbol{\beta}) \ , \tag{27}$$

where $\boldsymbol{\beta} = \frac{\mathbf{U}}{\Delta \mathbf{X}} \equiv \left(\frac{U^1}{\Delta X^1}, .., \frac{U^M}{\Delta X^M} \right)$ is an effective Courant number vector (recall that $\Delta \tau = 1$), and the finite difference flux-divergence operator $\mathcal{AS}$ identifies an advection scheme defined by its particular dependence on the values of ϕ and $\boldsymbol{\beta}$ available on the mesh in a neighborhood of the $\mathbf{x_i}$ grid point. The truncation error of the approximation in (27) represents the error of estimating ψ at the point of interest $\mathbf{x}_o$. Choosing an arbitrary grid point $\mathbf{x_i}$, that appears in the definition of the effective advecting velocity (25), as the closest grid point to $\mathbf{x}_o$,

$$\mathbf{x_i} = [\mathbf{x}_o] \equiv \left(NI(x_o^1/\Delta X^1) \cdot \Delta X^1, ..., NI(x_o^M/\Delta X^M) \cdot \Delta X^M \right) \tag{28}$$

(where NI denotes the nearest integer value), and using definitions (25) and (23), the resulting interpolation algorithm may be compactly written as

$$\psi(\mathbf{x}_o) = \psi([\mathbf{x}_o]) - \mathcal{AS}_{[\mathbf{x}_o]} \left(\psi, \frac{[\mathbf{x}_o] - \mathbf{x}_o}{\Delta \mathbf{X}} \right) . \tag{29}$$

Insofar as the linear, forward-in-time advection algorithms are concerned, there is no particular gain in using (29); indeed, the interpolation schemes derived from such algorithms may be obtained alternatively through more traditional arguments invoking the truncated Taylor expansion or, equivalently, polynomial fitting (cf. Smolarkiewicz and Grell, 1991). However, where preservation of the monotonicity and/or sign of the interpolated variable is concerned, the formula (29) becomes a useful tool as it allows us to implement advanced monotone and/or sign-preserving advection schemes in a simple and efficient manner. This simplicity and efficiency of (29) is a consequence of the *constancy* of the effective Courant number in (29), which allows for straightforward, alternate-direction (time-split) applications of one-dimensional advection schemes without degrading the formal accuracy of their constant coefficient limit [the alternative argument to that following (25)]. In contrast to fully multidimensional algorithms, the time-split approximations employing one-dimensional advection schemes have the virtue of considerable simplicity and versatility — the latter reflecting an availability of a great variety of attractive methods suitable for integration of the elementary one-dimensional, constant coefficient advection problem. Since by design

$$\underset{I}{\forall} \quad -\frac{1}{2} \leq \frac{[x_o^I] - x_o^I}{\Delta X^I} \leq \frac{1}{2} \,, \tag{30}$$

the computational stability is ensured for all (known to the author) one-dimensional forward-in-time advection schemes, securing thereby the stability of a time-split algorithm for an arbitrary M.

The utility of simple nonoscillatory schemes in (29) for semi-Lagrangian integrations of complex atmospheric problems is illustrated particularly well in the following example of a thermal convection. The governing system of equations consists of the momentum and temperature evolution equations for an ideal, nonrotating, two-dimensional Boussinesq fluid

$$\frac{d\mathbf{v}}{dt} = -\nabla\pi - g\frac{\Theta'}{\Theta_o}\nabla z \,, \tag{31a}$$

$$\frac{d\Theta}{dt} = 0 \,. \tag{31b}$$

Here, $\mathbf{v} = (u, w)$ is the velocity vector in the (x, z) vertical plane, π is the pressure departure from a hydrostatic value $\overline{\pi}(z)$ (both normalized by a reference density),

and g is the gravity. Θ denotes the potential temperature of a fluid parcel, whereas $\Theta' \equiv \Theta - \overline{\Theta}(z)$ represents its deviation from an ambient, hydrostatic profile $\overline{\Theta}(z)$; $\Theta_o = \overline{\Theta}(0)$ is a reference potential temperature. The prognostic equations (31a, b) are accompanied by the incompressibility constraint

$$\nabla \circ \mathbf{v} = 0 \ , \tag{32}$$

characteristic of the Boussinesq approximation. Free-slip, rigid-lid upper and lower boundaries, and open lateral boundaries are assumed.

The adapted semi-Lagrangian approximation to (31) and (32) consists of three distinct steps. First, departure points of the trajectories are evaluated using the second-order-accurate implicit midpoint rule

$$\mathbf{x}_o = \mathbf{x}_i - \Delta t \mathbf{v}\left(\mathbf{x}_m,\ t_m\right) \ , \tag{33}$$

where the velocities at the trajectories' midpoints $(\mathbf{x}_m,\ t_m)$ are predicted with the first-order-accurate integral of momentum equations

$$\mathbf{v}(\mathbf{x}_m, t_m) + O(\Delta t^2) = \tilde{\mathbf{v}}(\mathbf{x}_o, t_o) \equiv \mathbf{v}(\mathbf{x}_o, t_o) + \frac{1}{2}\Delta t \frac{d\mathbf{v}}{dt}(\mathbf{x}_o, t_o) \ . \tag{34}$$

The implicit nature of the trajectory algorithm consisting of (33) and (34) requires an iterative solution; the iterations converge providing

$$\mathcal{B} \equiv \| \frac{\partial \tilde{\mathbf{v}}}{\partial \mathbf{x}} \| \Delta t < 1 \ , \tag{35}$$

and one iteration (assuming the Euler backward approximation for the first guess) suffices for the second-order-accurate approximation to the departure points of trajectories (Smolarkiewicz and Pudykiewicz, 1991). In the second step of the semi-Lagrangian procedure, (31b, a) are approximated assuming the trapezoidal rule

$$\int_T \mathcal{R} dt \approx \frac{1}{2}\Delta t \big(\mathcal{R}(\mathbf{x}_i, t_o + \Delta t) + \mathcal{R}(\mathbf{x}_o, t_o)\big) \tag{36}$$

for evaluating the trajectory integral (19); updating the temperature prior to the momentum ensures availability of the buoyancy at $t + \Delta t$ in the vertical equation of motion. While integrating momentum equations (31a), pressure forces at $t + \Delta t$ are yet

unknown and must be determined from the constraint (32). In this third step of the procedure, the approximate solution to (31a) is written as

$$\mathbf{v}(\mathbf{x}_i, t+\Delta t) = \mathbf{v}^*(\mathbf{x}_i) - \frac{1}{2}\Delta t \nabla \pi(\mathbf{x}_i, t+\Delta t) \,, \tag{37}$$

where $\mathbf{v}^*(\mathbf{x}_i)$ combines all known terms appearing on the rhs of (36) [i.e., velocity, pressure gradient, and buoyancy terms evaluated at $(\mathbf{x}_o, t_o)$, as well as the buoyancy term at $(\mathbf{x}_i, t+\Delta t)$]. Applying (32) to (37) leads to the Poisson equation for pressure

$$\nabla^2 \pi(\mathbf{x}_i, t+\Delta t) = \frac{2}{\Delta t} \nabla \circ \mathbf{v}^*(\mathbf{x}_i) \,, \tag{38}$$

which is solved, subject to boundary conditions, using the standard FISHPACK software (Swarztrauber and Sweet, 1975). Having established pressure at $t+\Delta t$, (37) completes the procedure. The entire semi-Lagrangian algorithm for (31) and (32) is implicit with respect to all ODE integrations, ensuring thereby computational stability regardless of the time step employed; Δt is solely controlled by the convergence condition (35).

Figure 2a shows the actual solution to (31) and (32) obtained with the above-outlined solver which employs (29) in all interpolations inherent in semi-Lagrangian integrations. The $\mathcal{AS}$ operator is from the FCT advection scheme employed in the simple example, Fig. 1c, of the preceding section. The experimental set-up assumes a symmetric thermal of the initial radius $r_o = 250$ m; the thermal is placed in the $8r_o \times 8r_o$ domain resolved with 200×200 uniform grid intervals $\Delta X = \Delta Z = 0.04 r_o$. The center of the thermal is located at the vertical symmetry axis of the domain $r_o + \Delta Z$ above the bottom boundary. The thermal has a uniform, initial temperature excess of 0.5 K relative to the neutrally stratified environment of $\overline{\Theta}(z) = 300$ K. The Θ' field is shown after 7 characteristic time scales $T \equiv r_o/U$, where U is the characteristic velocity scale $U = \sqrt{2gBr_o}$ with B representing initial buoyancy of the thermal (Sánches et al., 1989). The time step of computations has been selected at $\Delta t \approx 0.06T$ [which results in $\mathcal{B} \approx 0.5$ in (35)].

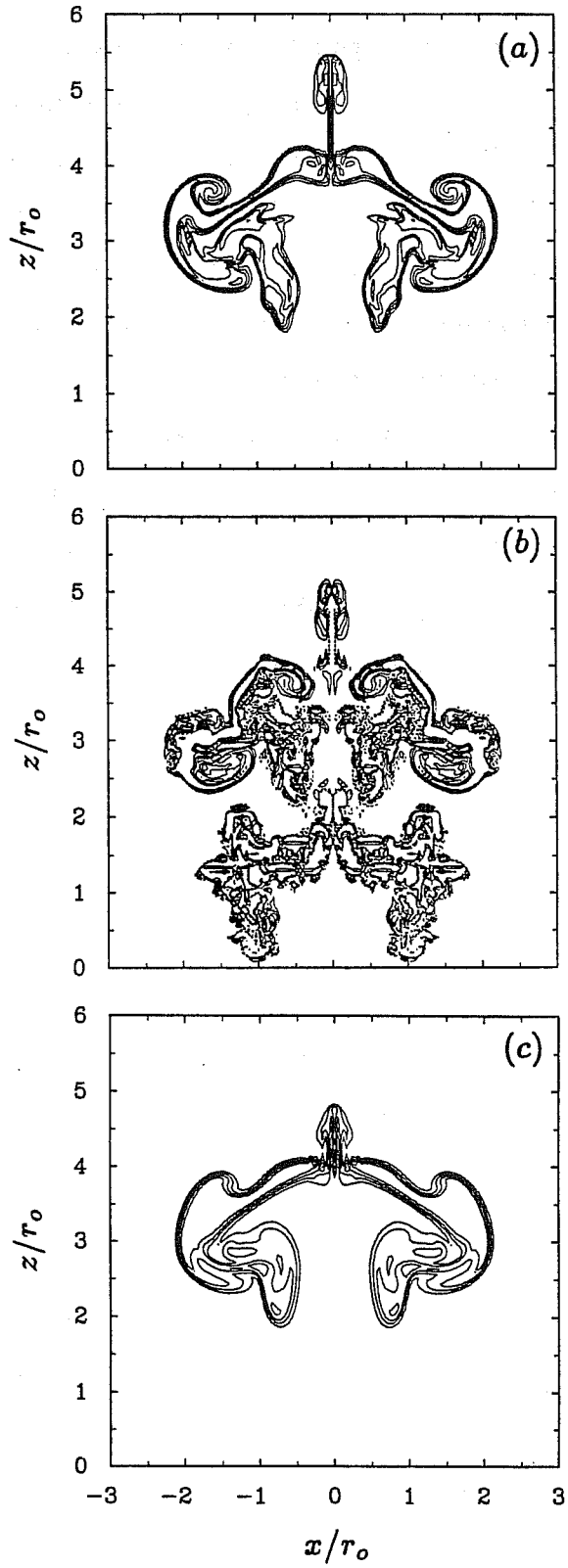

Figure 2. Isolines of the temperature perturbation Θ' of the inviscid buoyant thermal at dimensionless time $\tau \approx 7$ simulated with semi-Lagrangian model. The contour interval is 0.2 of the initial Θ' amplitude: a) experiment with nonoscillatory interpolation implementing FCT advection scheme in Fig. 1c; b) as in plate a) but with oscillatory interpolators; and c) as in plate b) but for the explicit Reynolds number 1500.

The excellent performance of the algorithm is evident in its ability to resolve fine interfacial structures and maintain sharp across-the-interface gradients while introducing no spurious oscillations. The highly inviscid yet smooth nature of computations is clear in Fig. 2a; the initial thermal's core may still be identified within narrow ($\sim 2\Delta X$ wide) interfacial convolutions engulfing ambient fluid. This performance is primarily controlled by the monotonicity of the interpolation procedure in (29), which by design preserves local convexity/concavity and sign, and ensures uniform boundedness, of the interpolated variables. In the absence of forcing, these properties hold along parcel trajectories consistently with analytic equations. Relaxation of the monotonicity constraint leads to poor results, evident in Fig. 2b displaying the "nonmonotone" (but otherwise equivalent to that in Fig. 2a) solution to the test problem. Although the overall appearance of the solution recalls that of Fig. 2a, the current scheme is incapable of reproducing a regular eddy pattern of the "monotone" result in Fig. 2a. Furthermore, it suffers from excessive numerical noise and exhibits a spurious secondary thermal in the wake of the main structure. The importance and utility of the monotonicity constraint are further emphasized in Fig. 2c, which shows the viscous (but otherwise equivalent to that in Fig. 2b) solution with the Reynolds and Prandtl numbers $Re = 2r_o U/\nu \approx 1500$ and $Pr = 1$, respectively. [Diffusion and heat conduction are introduced into the algorithm by an appropriate generalization of the forcing terms in (19).] Although inclusion of the explicit viscosity into the oscillatory algorithm eliminates the secondary wake thermal and most of the noise, the solution captures neither the strong interfacial gradients nor the fine-eddy structures evident in Fig. 2a [at $Re \approx 3000$, the solution (not shown) suffers from both the oscillations and unresolved eddy structures]. The three solutions discussed demonstrate that nonlinear, nonoscillatory techniques lead to results that are far superior to those generated with traditional linear methods. Due to the Lagrangian format of the approximated equations, the monotonicity constraint is ultimately imposed along a parcel trajectory, gaining thereby a deeper physical meaning than that from nonoscillatory Eulerian approximations. Parallel to the nonlinear stability issue, this constraint addresses topological and predictability issues by suppressing spurious oscillations of computed trajectories and preventing a trajectory intersection due to inadequacy of numerical approximations (see Smolarkiewicz and Pudykiewicz, 1991, for further discussion of

this particular issue as well as other aspects of semi-Lagrangian approximations for atmospheric fluids).

5. CONCLUDING REMARKS

The topics discussed in this paper cover only a part of an abundance of theoretical and practical issues associated with modern nonoscillatory advection schemes. While selecting the material for this lecture, I was mostly concerned with providing to the reader universal approaches that achieve their claimed accuracy regardless of the complexity of addressed flows. Keeping in mind that advection alone is seldom of interest to practical applications, and that it usually represents an element of a more complex problem, I have focused attention on variable-coefficient, multidimensional methods while neglecting to mention a variety of attractive one-dimensional transport schemes. True, one-dimensional schemes can be implemented in multiple dimensions by invoking directional splitting. This, however, is complex enough (if at least the second-order accuracy for arbitrary flows is going to be maintained) to warrant a separate paper. Instead, I have outlined the alternative of how to design easily at least a second-order-accurate model for an arbitrary fluid system using those nonoscillatory advection schemes which were originally designed for a one-dimensional constant-coefficient advection problem. This and the accompanying paper in this volume are intended to complement each other and provide the reader with the essential information needed to build simple yet effective, either Eulerian or semi-Lagrangian finite-difference models for a variety of atmospheric applications.

REFERENCES

Arakawa, A., 1966: Computational design for long-term numerical integration of the equations of fluid motions: Two-dimensional incompressible flow. *J. Comput. Phys.*, **1**, 119–143

Boris, J. P., and D. L. Book, 1973: Flux-Corrected Transport I: SHASTA — a fluid transport algorithm that works. *J. Comput. Phys.*, **11**, 38–69.

Grabowski, W. W., and P. K. Smolarkiewicz, 1990: Monotone finite-difference approximations to the advection-condensation problem. *Mon. Wea. Rev.*, **118**, 2082–2097.

Harten, A., J. M. Hyman, and P. D. Lax, 1976: On finite-difference approximations and entropy conditions for shocks. *Comm. Pure Appl. Math.* **29**, 297–322.

——, 1983: High resolution schemes for hyperbolic conservation laws. *J. Comput. Phys.*, **49**, 357–393.

Hirt, C. W., A. A. Amsden, and J. L. Cook, 1974: An arbitrary Lagrangian-Eulerian computing method for all flow speeds. *J. Comput. Phys.*, **14**, 227–253.

Merriam, M. L., 1989: An entropy-based approach to nonlinear stability. Ames Research Center, Report # NASA TM-101086, 143 pp.

Sánches, O., D. J. Raymond, L. Libersky, and A. G. Petschek, 1989: The development of thermals from rest. *J. Atmos. Phys.*, **46**, 2280–2292.

Smolarkiewicz, P. K., 1984: A fully multidimensional positive definite advection transport algorithm with small implicit diffusion. *J. Comput. Phys.*, **54**, 325–362.

——, and T. L. Clark, 1986: The multidimensional positive definite advection transport algorithm: Further development and applications. *J. Comput. Phys.*, **67**, 396–438.

——, and W. W. Grabowski, 1990: The multidimensional positive definite advection transport algorithm: Nonoscillatory option. *J. Comput. Phys.*, **86**, 355–375.

——, and P. J. Rasch, 1991: Monotone advection on the sphere: An Eulerian versus semi-Lagrangian approach. *J. Atmos. Sci.*, **48**, 793–810.

——, and G. A. Grell, 1991: A class of monotone interpolation schemes. *J. Comput. Phys.*, submitted.

——, and J. A. Pudykiewicz, 1991: A class of semi-Lagrangian approximations for fluids. *J. Atmos. Sci.*, submitted.

Staniforth A., and J. Côté, 1991: Semi-Lagrangian integration schemes for atmospheric models — A review. *Mon. Wea. Rev.*, in press.

Swarztrauber, P., and R. Sweet, 1975: Efficient FORTRAN subprograms for the solution of elliptic equations. NCAR TN/IA-109, July, 138 pp.

Sweby, P. K., 1984: High resolution schemes using flux limiters for hyperbolic conservation laws. *SIAM J. Numer. Anal.*, **21**, 995–1011.

Tremback, C. J., J. Powell, W. R. Cotton, and R. A. Pielke, 1987: The forward-in-time upstream advection scheme: Extension to higher orders. *Mon. Wea. Rev.*, **115**, 540–555.

Zalesak, S. T., 1979: Fully multidimensional flux-corrected transport algorithms for fluids. *J. Comput. Phys.*, **31**, 335–362.

——, 1987: A preliminary comparison of modern shock-capturing schemes: Linear advection. *Advances in computer methods for partial differential equations*, Vol. VI, R. Vichnevetsky and R. Stepleman (editors), IMACS, 565 pp.